# Science research writing for non-native speakers of English

*Yang Yirun* 1024041132
*School of Computer Science*
*Nanjing University of Posts and Telecommunications*
*Nanjing China*

## I. THEORETICAL FRAMEWORK

The fundamental modes of heat transport in an aluminum rod can be characterized by a parabolic partial differential equation, the *heat equation*[1],

$$\frac{\partial u}{\partial t} - \alpha\frac{\partial^2 u}{\partial x^2} + \beta(u - u_{air}) + \gamma(u^4 - u_{air}^4) = 0. \quad (1)$$

Where $\alpha = \frac{\kappa}{\rho c_{Al}}$, $\rho$ is the density of aluminum, $\beta = \frac{2h_c(L+r)}{\rho c_{Al} r}$, $r$ is the radius of the aluminum rod, $L$ is the total length of the rod, and $\gamma = \frac{2\epsilon\sigma(L+r)}{\rho c_{Al} r}$, $\sigma$ is the Stefan-Boltzmann constant, which is assumed in this paper to be, $\sigma = 5.670373 \times 10^{-8}\ \mathrm{Wm^{-2}K^{-4}}$. Equation 1 describes the distribution of heat (or variation in temperature) in a given region over time undergoing all three modes of heat transport. For this paper, $u = u(x, t)$ will be the temperature at point, $x$ and time, $t$.

The solution to equation 1 (with the proper boundary conditions) fully describes both the transient phase of the effect of heat flow and temperature change and the static (equilibrium) phase of the same. However, analytically solving equation 1 is difficult. Thus, it is useful to isolate and develop a heat flow model each of the fundamental modes of heat transfer and consider them separately.

The following discussion of the three modes of heat transport were taken into consideration whilst designing the experiments (see Section II).

### A. Conduction

Isolating conduction greatly reduces the complexity of equation 1, since the convection and radiation terms are removed,

$$\frac{\partial u}{\partial t} - \alpha\frac{\partial^2 u}{\partial x^2} = 0. \quad (2)$$

Equation 2 describes the time and spacial evolution of temperature in the aluminum rod subjected to certain boundary conditions. During experimentation, the end of the rod is heated with a constant power source which is delivering heat energy. Since the amount of heat energy per unit time, $\frac{dQ}{dt}$ is known, it is convenient to view conduction in the following form,

$$\frac{dQ}{dt} = -\kappa A_\times \frac{du}{dx}. \quad (3)$$

Where $A_\times$ is the cross sectional area. Equation 3 describes the amount of heat energy transported between two points on the rod. Note it is now clear to see that the unit of $\kappa$ is $\mathrm{Wm^{-1}K^{-1}}$. The negative sign is indicative of the direction of heat transfer. For simulations, the discrete form of equation 3 is used (see Appendix **??**). The relationship between equation 2 and 3 is given by the specific heat equation,

$$\frac{dQ_{net}}{dt} = (c_{Al}\rho dV)u_{rise}. \quad (4)$$

Where $\frac{dQ_{net}}{dt}$ is the *net* heat transfer through an infinitesimal volume segment of the rod, and $u_{rise}$ is the corresponding temperature increase of that point. So, using 3 and 4 one can derive 2.

Furthermore, there exists a finite contact thermal resistance between the heat-power source and the aluminum rod. Using the discrete form of equation 3, the absolute thermal resistance between multi-layered contact systems can be determined with,

$$\frac{\Delta Q}{\Delta t} = -\frac{(u_1 - u_2)}{\frac{\frac{\Delta x_1}{\kappa_1} + \frac{\Delta x_2}{\kappa_2} + \cdots + \frac{\Delta x_n}{\kappa_n}}{A_\times}} = -\frac{\Delta u}{R_{th}}. \quad (5)$$

Where $\Delta x_i, \kappa_i$ are the length and conductivities of the multiple layers between the heat source and end of the aluminum rod. Practically, to determine $R_{th}$, a parameter $P_{in}$ is introduced, which is the amount of heat flow that is going through the rod.

### B. Convection

Considering convection separately equation 1 becomes,

$$\frac{\partial u}{\partial t} = -\beta(u - u_{air}). \quad (6)$$

Equation 6 describes the change in temperature due to a differential in the rod and air temperature. A differential in rod and air temperature facilitates heat exchange. The heat exchange is governed by,

$$\frac{dQ}{dt} = h_c A_\ominus (u - u_{air}), \quad (7)$$

and one can derive equation 6 with equation 7 by relating them by equation 4. In equation 7, $A_{\ominus}$ is the surface area of convection. Also, the units of $h_c$ can be seen to be, $\mathrm{Wm^{-2}K^{-1}}$. It is important to note that equation 7 is a simplification of convective heat flow. The convective coefficient, $h_c$ has geometrical and temperature dependence, but for the purposes of this paper the temperature dependence is neglected. For situations in which the rod is vertical, compared to when the rod is horizontal, the values of $h_c$ differ. This geometrical dependence; the fact that hot air is less dense than cold air, so the rising of hot air in the two different situations (and anything in between) are different, which effects the value of $h_c$.

Furthermore, one can see that equation 6 simplifies to an ordinary differential equation[2]. The solutions to equation 6 are in the form,

$$u(t) = u_{air} + (u_0 - u_{air})\mathrm{e}^{-\beta t}. \tag{8}$$

Where $u_0$ is the initial temperature of the aluminum rod.

## II. EXPERIMENTAL SETUP

In preparation for all experiments, circuits to amplify the calibrated thermocouple readings and software code for MATLAB-Arduino integration were established. The experiments conducted are summarized in Table I.

TABLE I: Experiment number and the corresponding heat transfer parameters to be found.

| Experiment number | Type of experiment | Parameters from fit |
|---|---|---|
| 1 | pure conduction | $\kappa$, $c_{Al}$, $P_{in}$ |
| 2 | convection bare rod | $h_c$, $c_{Al}$, $\epsilon$ |
| 3 | coupled conduction and convection bare rod | $\kappa$, $c_{Al}$, $h_c$, $\epsilon$, $P_{in}$ |
| 4 | convection black rod | $h_c$, $c_{Al}$, $\epsilon$ |
| 5 | coupled conduction and convection black rod | $\kappa$, $c_{Al}$, $h_c$, $\epsilon$, $P_{in}$ |

## III. RESULTS AND DISCUSSION

For each individual experiment, the raw data collected was compared to a simulation that matched the experiment. The simulation used a finite difference method of solving either equations 1, 2, 6, with the appropriate boundary conditions. Then, using MATLAB, a least-squared fitting technique was carried out in order to determine the parameters in which the simulation best matched the data. In order to initiate the simulation, initial guesses for the heat transport parameters, $c_{Al}$, and $P_{in}$ were needed. Table II summarizes the initial values inputted for the simulation.

TABLE II: Simulation parameter values.

| Parameter | Value | Source |
|---|---|---|
| Length | 0.3048 m | Measurement |
| Diameter | 0.0225 m | Measurement |
| Rod segments | 10 | Parameter Optimization |
| $T_{room}$ | 20°C | TMP35 sensor |
| Density | 2709 $\mathrm{kgm^{-3}}$ | Measurement |
| $c_{al}$ | 900 $\mathrm{Jkg^{-1}K^{-1}}$ | see Ref. 3 |
| $\kappa$ | 205 $\mathrm{Wm^{-1}K^{-1}}$ | see Ref. 4 |
| $h_c$ | 10 $\mathrm{Wm^{-1}K^{-2}}$ | see Ref. 5 |
| $\epsilon_{bare}$ | 0 | Approximation |
| $\epsilon_{black}$ | 1 | Approximation |
| $P_{in}$ | varies between experiments | Approximation |

### 1. *Pure conduction*

Initially, it was found that the temperature of the rod was not reaching the levels predicted by the simulation. To account for the discrepancy in rod temperatures, it was found to be that all the power that the heat source outputted did go into the rod. Insulation was added to the heat source to rectify the discrepancy and bring the measured data closer to the idealized simulation.

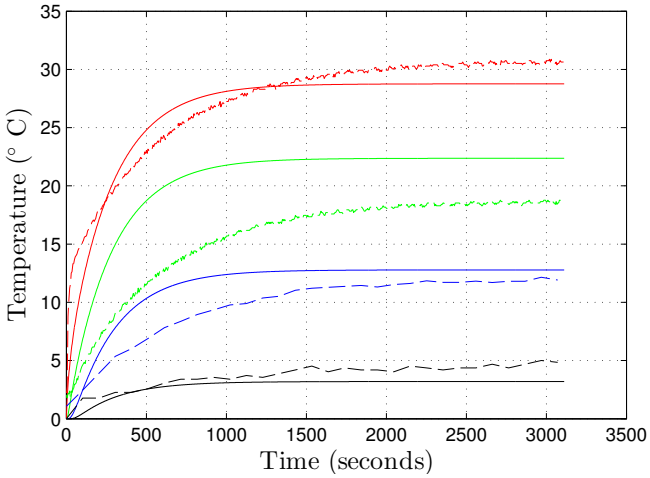


FIG. 1: Results of fitted plot to data. Solid lines represent the simulation and dashed lines represent the raw data. **Red** corresponds to $x = 0.00$ m, **green** to $x = 0.075$ m, **blue** to $x = 0.15$m and **black** to $x = 0.225$ m. Heat source is located at $x = 0.00$ m, as described in Section.

Figure 1 displays the raw data against the least-

squared fitted simulation data. It is important to note that only the thermocouples placed at $x = 0.15$ m and $x = 0.225$ m were used to produce the fitted results. These thermocouples were deemed to be properly calibrated and at a location where no externalities can effect their measurements. However, note that there still exists a discrepancy for the fitted thermocouples against the simulated data. This discrepancy is to be expected as the contact between thermocouples and rod is imperfect and the effect of insulation was not taken into consideration in the simulation. Both of these sources of error imply that the corresponding assumptions made in Section **??** were incorrect. The remaining two thermocouples had large errors associated with them which can be easily seen on figure 1. The thermocouple located at $x = 0.00$ m measures a temperature higher than the simulation. After careful investigation, this error was deemed to be expected because that thermocouple was placed directly in contact with both the heat source and aluminum rod. This location enables the thermocouple to reach a greater equilibrium temperature than the rod. Furthermore, the thermocouple located at $x = 0.075$ m is completely in disagreement with the simulation. It was deemed that the calibration of this thermocouple was flawed.

The the simulated fit result in the heat transfer parameters of:

$$\begin{aligned} &\kappa = 203.96 \text{ Wm}^{-1}\text{K}^{-1} \\ &c_{Al} = 945.31 \text{ Jkg}^{-1}\text{K}^{-1} \\ &P_{in} = 10.37 \text{ W} \end{aligned}$$

### 2. *Convection with bare rod*

The following section will provide results on the two experiments outlined in section 99.

**Experiment A:**

As described in Section 7 the entire bar was chilled to a uniform temperature of $\approx 5°$C and heated up to a temperature of $\approx 20°$C. Figure 2 displays the raw data against the least squared fitted simulation data. There is only one resultant fit because the theory discussed in section I B implies that there is no $x$ dependence on convective heat transfer. From this, it can be concluded that the convective transfer coefficient, $h_c$ is also independent of the location on the rod (for a horizontal geometry).

The the simulated fit result in the heat transfer parameters of:

$$\begin{aligned} &h_c = 12.00 \text{ Wm}^{-2}\text{K}^{-1} \\ &c_{Al} = 925.53 \text{ Jkg}^{-1}\text{K}^{-1} \\ &\epsilon = 0.200 \end{aligned}$$

The average error between the thermocouples and the simulated fit data is 0.0228°C, which is within reasonable experimental uncertainty. Note, two thermocouples ($x = 0.075$ m and $x = 0.225$ m) were ignored as their temperature readings were unreliable due to miscalibration. This complication does not effect the integrity of the results because it is known from Section I B that all the thermocouples should theoretically produce the same curve.

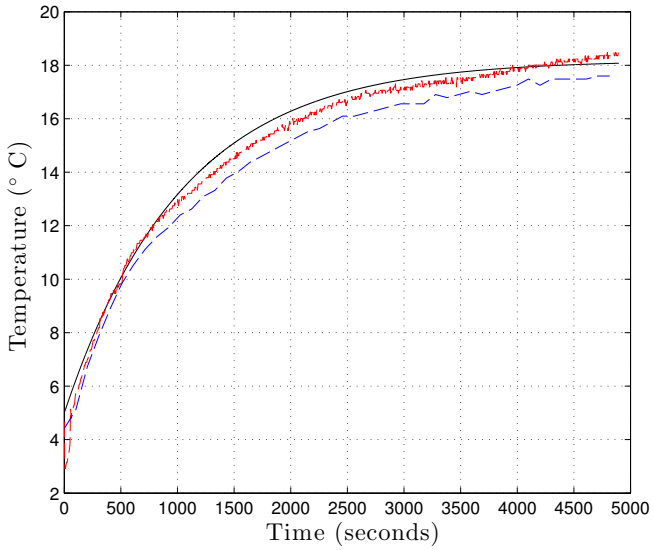


FIG. 2: Results of fitted plot to data. Solid **black** line represents the result from the fitted simulation and dashed lines represent the raw data from the thermocouples. **Red** corresponds to $x = 0.00$ m, **blue** to $x = 0.15$ m.

Furthermore, the thermocouples in figure 2 both record a temperature lower than the simulation. This phenomenon can be explained by the fact that the thermocouples may conduct heat from the tip of the measurement probe, therefore producing a measurement for the temperature that is lower than the temperature of the rod. This conclusion leaves the corresponding assumption made for experiment A in Section 99 moot.

**Experiment B:**

As described in Section 99 the entire bar was heated to a uniform temperature of $\approx 55°$C and heated up to a temperature of $\approx 20°$C. Figure 3 displays the raw data against the least squared fitted simulation data. There is only one resultant fit because the theory discussed in section I B implies that there is no $x$ dependence on convective heat transfer.

The the simulated fit result in the heat transfer parameters of:

$$\begin{aligned} &h_c = 11.54 \text{ Wm}^{-2}\text{K}^{-1} \\ &c_{Al} = 899.76 \text{ Jkg}^{-1}\text{K}^{-1} \\ &\epsilon = 0.199 \end{aligned}$$

The average error between the thermocouples and the simulated fit data is 0.0214°C, which is within reasonable experimental uncertainty. Note, one thermocouple

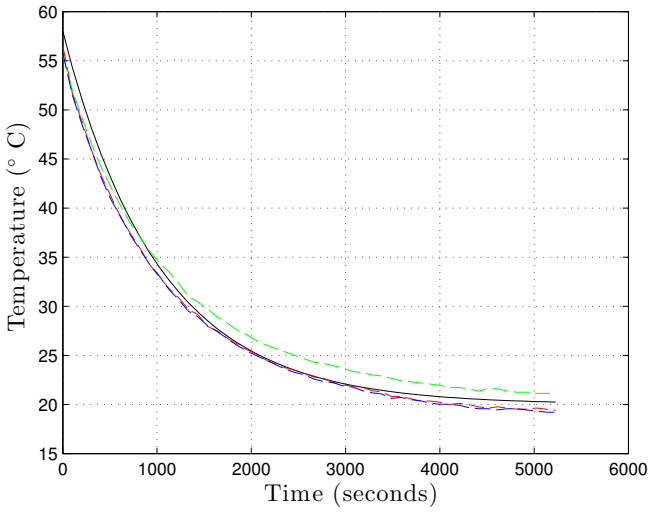


FIG. 3: Results of fitted plot to data. Solid **black** line represents the result from the fitted simulation and dashed lines represent the raw data from the thermocouples. **Red** corresponds to $x = 0.00$ m, **green** to $x = 0.075$ m, and **blue** to $x = 0.15$ m.

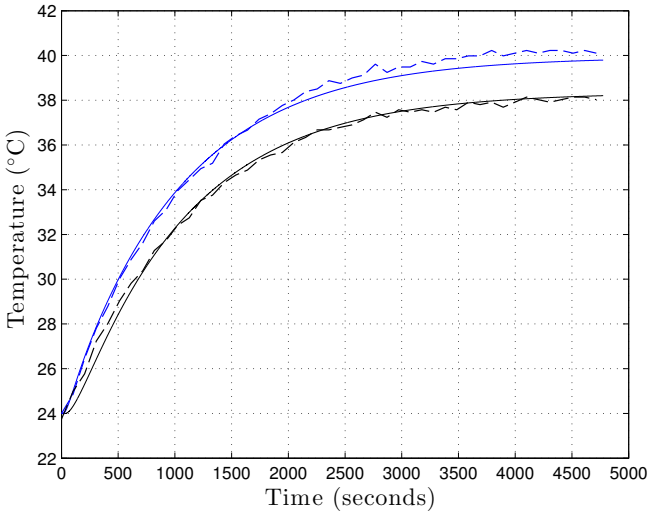


FIG. 4: Results of fitted plot to data. Solid lines represent the simulation and dashed lines represent the raw data. **Blue** to $x = 0.15$m and **black** to $x = 0.225$ m. Heat source is located at $x = 0.00$ m, as described in Section 100.

($x = 0.225$ m) was ignored as its temperature readings were unreliable due to mis-calibration. This complication does not effect the integrity of the results because it is known from Section I B that all the thermocouples should theoretically produce the same curve.

Furthermore, the thermocouples in figure 2 show a minimal amount of discrepancy with respect to the simulation fit. This discrepancy is expected, since the method the bar was heated, explained in Section **??**, is flawed. The method may create a small temperature differential inside the bar, allowing some conduction to occur. This conduction is responsible for the slight discrepancies.

### *3. Coupled conduction and convection with bare rod*

As described in Section 100, all three fundamental modes of heat transport were analyzed for a bare rod. Figure 4 displays the raw data against the least squared fitted simulation data. The

The fitted simulation yields the physical parameters:

$$\begin{aligned}
&\kappa = 185.32 \text{ Wm}^{-1}\text{K}^{-1} \\
&h_c = 11.90 \text{ Wm}^{-2}\text{K}^{-1} \\
&\epsilon = 0.231 \\
&c_{Al} = 930.02 \text{ Jkg}^{-1}\text{K}^{-1} \\
&P_{in} = 4.998 \text{ W}
\end{aligned}$$

The average error from the simulation lines to the three thermocouple data sets is 0.1036°C, which is within reasonable experimental uncertainty. Two thermocouples ($x = 0.00$ m and $x = 0.075$ m) were ignored as their temperature readings were unreliable due to mis-calibration. The impact of two unreliable thermocouples was insignificant. The two reliable thermocouples were enough to generate simulated fit parameters that matched those of previous experiments. Furthermore, figure 4 shows minimal discrepancy and can be accredited to noise.

Using the $P_{in}$ parameter determined from the fit (see figure 4), equation 5, the thermal contact resistance between the heat source [6], thermal paste [7] and aluminum rod system was, $\boxed{R_{th} = 3.14 \text{ KW}^{-1}}$.

## Summary of Results

Compiling all the results in Section III and determining their inherent, experimental relative errors (table III) and with respect to accepted values of the heat transfer parameters, table III is established.

TABLE III: Summary of all the fitted results and their respective relative errors from the furthest empirically obtained value.

| Parameter | Value |
|---|---|
| $\kappa$ | $214.34 \pm 18.40\%$ $\text{Wm}^{-1}\text{K}^{-1}$ |
| $h_c$ | $12.02 \pm 6.00\%$ $\text{Wm}^{-2}\text{K}^{-1}$ |
| $\epsilon_{bare}$ | $0.210 \pm 10.00\%$ |
| $\epsilon_{black}$ | $0.867 \pm 6.46\%$ |
| $c_{Al}$ | $945.23 \pm 4.81\%$ $\text{Jkg}^{-1}\text{K}^{-1}$ |
| $R_{th}$ | $3.503 \pm 11\%$ $\text{KW}^{-1}$ |

### Discussion

As tables III and IV depict, there are two different types of errors that one can reason about. Most of these errors were outlined with the results in Section III, as a summary:

- Small errors in thermocouple calibrations propagating through amplifier circuits.
- No model of insulation in simulation, which leads to errors in fitting.
- Errors in unwanted heat transfer mechanisms. For example, having conduction heat transfer contributions in the pure convection and radiation experiments.
- Small errors in thermal resistance can be taken into account by the fact that uneven amounts can be applied (or the same amount is not applied each experiment).
- Thermocouples conducting heat from the rod, thus lowering the temperature measurement.
- Room temperature fluctuations may cause errors (day and night temperature fluctuations).

## IV. CONCLUSION

Improvements can be made for future experimentation. Possible improvements would include increasing the accuracy of temperature measurements. This improvement would include: higher quality thermocouples and an improved method to secure the thermocouples onto the rod. A more sophisticated modeling process would improve simulation results since it will model the real situation closer than the 1-D approximation done in this paper. Additionally, carrying out the experiment in a more controlled environment would help reduce noise, temperature fluctuations and unwanted non-linear effects from the surroundings. Inside the laboratory, there can be many sources of thermodynamic heat transfer processes occurring such as: movement of humans, air conditioning, pressure, humidity, day and night temperature. If one can control as many of these as possible, a characteristic value for the heat transfer parameters can be better determined.

In closing, the heat transport parameters: thermal conductivity, $\kappa$ , the convective coefficient of the system $h_c$, emissivity of a bare, sand-blasted aluminum rod, $\epsilon_{bare}$ and emissivity of a spray-painted black aluminum rod, $\epsilon_{black}$ were determine, as well as, the specific heat capacity $c_{Al}$ and thermal contact resistance with an LTO100 power resistor, $R_{th}$. These values were obtained in a fairly accurate manner. Finally, the three fundamental modes of heat transport: conduction, convection, and radiation were discussed an analyzed for an aluminum rod.

TABLE IV: Summary of all the fitted results and their respective relative errors from the accepted value. See Ref. 3, 4, 5, 8 for accepted values.

| Parameter | Value | Actual Value |
|---|---|---|
| $\kappa$ | $214.34 \pm 4.56\%$ $\mathrm{Wm^{-1}K^{-1}}$ | 205 $\mathrm{Wm^{-1}K^{-1}}$ |
| $h_c$ | $12.02 \pm 20.20\%$ $\mathrm{Wm^{-2}K^{-1}}$ | 10 $\mathrm{Wm^{-2}K^{-1}}$ |
| $\epsilon_{bare}$ | $0.210 \pm 10.00\%$ | 0.210 |
| $\epsilon_{black}$ | $0.867 \pm 6.46\%$ | 0.867 |
| $c_{Al}$ | $945.23 \pm 5.03\%$ $\mathrm{Jkg^{-1}K^{-1}}$ | 900 $\mathrm{Jkg^{-1}K^{-1}}$ |
| $R_{th}$ | 3.503 $\mathrm{KW^{-1}}$ *error not applicable* | *not applicable* |

[1] The heat equation mentioned is the one dimensional form. The full form of the heat equation has three spacial dimensions, but is outside the scope of this paper.

[2] Convection cooling and heating is sometimes called Newton's Law of Cooling and Heating, in cases where the heat transfer coefficient is independent or relatively independent of the temperature difference between object and environment.

[3] "Specific heats and molar heat capacities for various substances at 20 c," http://hyperphysics.phy-astr.gsu.edu/hbase/tables/sphtt.html, accessed: 2014-07-02.

[4] "Thermal conductivity," http://hyperphysics.phy-astr.gsu.edu/hbase/tables/thrcn.html, accessed: 2014-07-01.

[5] "Heat transfer mechanisms," http://www.engr.colostate.edu/~allan/heat_trans/page4/page4.html, accessed: 2014-07-04.

[6] "Power resistor thick film technology: Lto100 power resistor," http://www.vishay.com/docs/50051/lto100.pdf, accessed: 2014-07-06.

[7] "Tgreasetm 2500 series thermal grease," lairdtech.com/WorkArea/DownloadAsset.aspx?id=1907, accessed: 2014-07-06.

[8] "Specific heats and molar heat capacities for various substances at 20 c," http://hyperphysics.phy-astr.gsu.edu/hbase/tables/sphtt.html, accessed: 2014-07-06.